

Detecting many-body Bell non-locality by solving Ising models

Irénée Frérot^{1,2*} and Tommaso Roscilde^{3†}

¹ *ICFO-Institut de Ciències Fotoniques, The Barcelona Institute of Science and Technology, Av. Carl Friedrich Gauss 3, 08860 Barcelona, Spain*

² *Max-Planck-Institut für Quantenoptik, D-85748 Garching, Germany and*

³ *Laboratoire de Physique, CNRS UMR 5672, Ecole Normale Supérieure de Lyon, Université de Lyon, 46 Allée d'Italie, Lyon, F-69364, France*

Bell non-locality represents the ultimate consequence of quantum entanglement, fundamentally undermining the classical tenet that spatially separated degrees of freedom possess objective attributes independently of the act of their measurement. Despite its importance, probing Bell non-locality in many-body systems is considered to be a formidable challenge, with a computational cost scaling exponentially with system size. Here we propose and validate an efficient variational scheme, based on the solution of inverse Ising problems, which in polynomial time can probe whether an arbitrary set of quantum data is compatible with a local theory; and, if not, it delivers a many-body Bell inequality violated by the quantum data. We use our approach to unveil new many-body Bell inequalities, violated by suitable measurements on paradigmatic quantum states (the low-energy states of Heisenberg antiferromagnets), paving the way to systematic Bell tests in the many-body realm.

Quantum correlations, such as entanglement [1], Einstein-Podolsky-Rosen correlations [2, 3] and Bell correlations [4, 5], are common features of microscopic ensembles of quantum degrees of freedom, such as the electronic and nuclear spins in atoms and molecules [6], or pairs of photons produced by parametric down-conversion [7]. The persistence of such correlations in many-body systems is a central issue, of both fundamental as well as technological interest: an obstruction to the scalability of quantum correlations would be the core feature of a putative quantum-to-classical transition [8, 9]; and, in parallel, scalable quantum correlations are the essential resource for most of the quantum technologies of second generation [10]. In view of all this, the robust certification of quantum correlations in many-body systems stands as a central problem for theoretical as well as experimental quantum physics.

The most robust certification scheme – namely, the one requiring the minimal amount of hypotheses – is undoubtedly offered by the so-called *device-independent* (DI) approach, relying on the violation of a Bell inequality, which does not assume anything about the quantum device except what can be controlled or assessed experimentally. To be specific, in the following we shall assume that a quantum many-body system is composed of N spatially separated degrees of freedom – that we will imagine as arranged over a lattice – on which k different observables (*inputs*) can be experimentally measured; and each of the observables can deliver p results (*outputs*). We shall indicate with $\sigma_a^{(i)}$ the p possible values of the a -th observable ($a = 0, \dots, k-1$) on the i -th degree of freedom ($i = 1, \dots, N$), corresponding to p eigenvalues of the quantum operator $\hat{M}_a^{(i)}$ – these choices define a (N, k, p) scenario for a Bell test (Fig. 1A). In practice within a DI approach one does not require the knowledge of the actual quantum operators $\hat{M}_a^{(i)}$, and the very Hilbert space dimension associated

to the N degrees of freedom may be ignored. Moreover, we will indicate with $\langle f(\sigma) \rangle_Q$ (where $\sigma = \{\sigma_a^{(i)}\}$) any function f of the measurement outputs, averaged over repeated measurements on the quantum system – hereafter denoted as quantum data. Typically, f is the product of a subset of the measurement outputs, so that the quantum data consists of a collection of correlation functions measured on the quantum device.

In this context, the DI approach certifies the strongest form of quantum correlations – Bell non-locality – when the quantum data violate a Bell inequality [4, 5], namely a constitutive relationship for all local-variable (LV) models, designed to capture the most general form of classical correlations. First envisioned by Bell [11], such models are defined by the existence of a joint probability distribution for all the measurement outcomes [12], $P_{LV}(\sigma)$. In other words, in LV models, the measurement outputs $\{\sigma_a^{(i)}\}$ are treated as classical variables, randomly sampled from P_{LV} in each experimental run – very much like in classical physics, where the system is always in an objectively existing microstate, belonging to a statistical distribution which solely expresses our ignorance on such a state. If $[\hat{M}_a^{(i)}, \hat{M}_b^{(i)}] \neq 0$, such a joint probability distribution for $\sigma_a^{(i)}$ and $\sigma_b^{(i)}$ is not admitted by quantum mechanics, creating a fundamental tension between the latter and LV models. In the following we shall indicate with $\langle \dots \rangle_{LV}$ an average over the P_{LV} distribution. The simplest Bell inequalities constraining the predictions of LV models are linear combination of few-body expectation values:

$$\sum_{i=1}^N \sum_{a=1}^k \alpha_a^{(i)} \langle \sigma_a^{(i)} \rangle_{LV} + \sum_{i < j} \sum_{a,b=1}^k \beta_{a,b}^{(i,j)} \langle \sigma_a^{(i)} \sigma_b^{(j)} \rangle_{LV} + \dots \geq -B_c \quad (1)$$

where $-B_c$ is the so-called classical bound. Geometrically, every such inequality defines a hyperplane in the space of correlations, separating two half-spaces, one of which contains all data sets compatible with LV models. The intersection of these half-spaces defines the so-called local polytope (Fig. 1B). Certifying Bell non-locality corresponds then to assessing that the quantum data of interest lie outside the local polytope, violating the Bell inequality defining the closest

*Electronic address: irenee.frerot@icfo.eu

†Electronic address: tommaso.roskilde@ens-lyon.fr

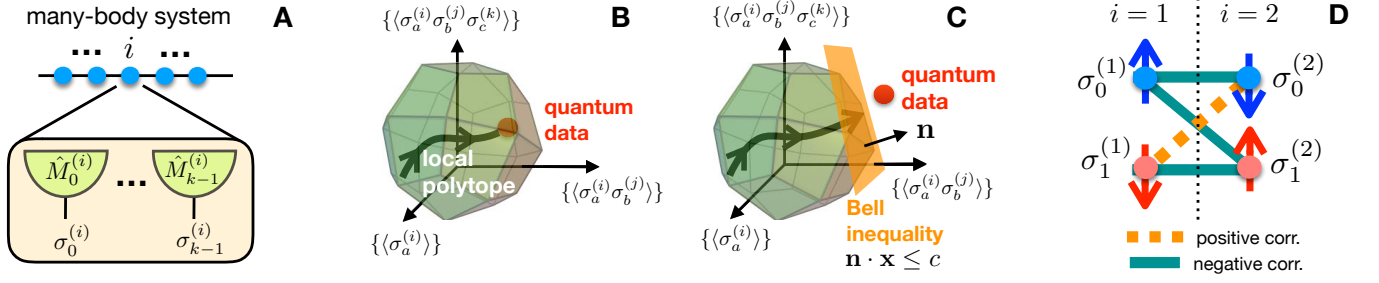


FIG. 1: **Variational search of local-variable models.** (A) Sketch of the generic (N, k, p) setting for Bell tests: each degree of freedom of a quantum many-body system is subject to the measurement of k different operators \hat{M}_a , with p different outcomes σ_a for each measurements; (B) Our Bell test of a set of quantum data – comprising arbitrary moments $(\langle \sigma_a^{(i)} \rangle, \langle \sigma_a^{(i)} \sigma_b^{(j)} \rangle, \text{etc.})$ of the statistics of the measurement outcomes – consists of generating a family of local-variable (LV) models which approximate the quantum data at best, describing a trajectory (black line) within the local polytope bounding all predictions of LV models; (C) if the LV predictions maintain a finite distance from the quantum data, this reveals the existence of a Bell inequality (corresponding to the closest polytope facet) which the quantum data violate; (D) Frustrated correlation pattern among local variables in a $(2,2,2)$ setting, which an LV model should reproduce in order to realize the correlations of a Bell pair $(|\uparrow_1 \downarrow_2\rangle - |\downarrow_1 \uparrow_2\rangle) / \sqrt{2}$.

facet to the quantum data themselves (Fig. 1C).

The search for Bell inequalities violated by quantum many-body data for systems with $N \gg 1$ represents a formidable task. Indeed, given a quantum data set $\{\langle f_r(\sigma) \rangle_Q; r = 1, \dots, R\}$ – where the f_r are arbitrary functions of the measurement outputs (such as n -point correlation functions) – the local polytope has p^{kN} vertices, and its full reconstruction has therefore a prohibitive (exponential) cost [4]. Many-body Bell inequalities have been successfully identified in the past [13–15], but they are violated only by selected quantum states [16]. More systematic strategies have been devised recently that either restrict the search to Bell inequalities which are fully symmetric under exchange of lattice-site indices (namely with $\alpha_a^{(i)} = \alpha_a, \beta_{a,b}^{(i,j)} = \beta_{a,b}$, etc. in Eq. (1)) [17], circumventing the exponential cost but losing in generality; or that approximate the local polytope from the outside [18], with an exponential cost for the approximation to converge to the exact polytope. Hence the *quantum membership problem* (“Does a set of quantum data belong to the local polytope?”) is considered to be an exponentially hard one. Our main result is to exhibit an algorithm which solves such a problem in polynomial time under very general assumptions; and to validate such an approach by discovering new Bell inequalities violated by relevant quantum many-body states in the thermodynamic limit.

Our approach to the above problem consists of trying to explicitly build an LV model P_{LV} which reproduces the quantum data, namely a model fulfilling the following

$$\text{conditions : } \langle f_r(\sigma) \rangle_{LV} = \langle f_r(\sigma) \rangle_Q \quad (r = 1, \dots, R) \quad (2)$$

(within the error bar of the quantum data, if the latter come with a finite uncertainty). In a realistic scenario, we assume that R scales polynomially with N ; therefore, if such a distribution exists, it is certainly not unique, because it can be parametrized by many more parameters ($p^{kN} - 1$ independent values) than the number R of constraints. Yet, if multiple distributions exist, there is one of them which is least biased, namely one that is parametrized by the *minimal* number of parameters required to satisfy the constraints: such a distribution

is the one that maximizes the Shannon entropy under the constraints [19, 20], namely the one minimising the “free-energy” functional

$$F[P_{LV}] = \sum_{\sigma} P_{LV} \log P_{LV} - \sum_r K_r (\langle f_r \rangle_{LV} - \langle f_r \rangle_Q) . \quad (3)$$

The minimum of the above functional is known to take the form of a Boltzmann distribution

$$P_{LV}(\sigma) = \exp[\sum_r K_r f_r(\sigma)] / \mathcal{Z} \quad (4)$$

in which the Lagrange multipliers K_r (forming the vector $\mathbf{K} = \{K_r\}$) play the role of the coupling constants defining an effective Hamiltonian $\mathcal{H}(\sigma; \mathbf{K}) = -\sum_r K_r f_r(\sigma)$, and \mathcal{Z} is the corresponding partition function. Therefore, our central observation is the following: if a LV model reproducing the quantum data exists, it can be found in the form of Eq. (4) upon adjusting the coupling constants. In the case of binary outcomes ($p = 2$), to which we will hereafter specialize, the σ ’s are Ising variables ($\sigma = \pm 1$), and therefore the LV model represents the equilibrium Boltzmann distribution of a generalized Ising model with Hamiltonian \mathcal{H} .

In summary, without loss of generality, the problem of reproducing the quantum data with an LV model is reduced to adjusting the coupling constants of an Ising model so as to fulfill the conditions Eq. (2). This, however, is a well-known problem in statistical inference, namely an *inverse Ising problem* [21], which has the remarkable feature of being a convex optimization problem upon introducing the following cost function:

$$\mathcal{L}(\mathbf{K}) = \log \mathcal{Z}(\mathbf{K}) - \sum_r K_r \langle f_r \rangle_Q \quad (5)$$

where \mathcal{L} is related to (minus) the so-called log-likelihood. Indeed, the Hessian of the cost function

$$H_{rs} = \frac{\partial^2 \mathcal{L}}{\partial K_r \partial K_s} = \langle f_r f_s \rangle_{LV} - \langle f_r \rangle_{LV} \langle f_s \rangle_{LV} \quad (6)$$

is the covariance matrix of the f_r functions, and it is therefore semi-definite positive. The convexity of the cost function implies that a simple gradient-descent algorithm, following the gradient $\mathbf{G} = \{G_r\}$ of the cost function:

$$G_r = \frac{\partial \mathcal{L}}{\partial K_r} = \langle f_r \rangle_{LV} - \langle f_r \rangle_Q, \quad (7)$$

is guaranteed to converge to the global minimum [22].

Our algorithm presents then two possible behaviors: 1) if the quantum data are reproducible by an LV model, the algorithm converges to well-defined couplings \mathbf{K} which lead to the vanishing of the gradient \mathbf{G} [Eq. (7)], namely of the distance vector between the quantum data and the LV predictions (Fig. 1B); 2) otherwise, the quantum data lie outside of the local polytope, so that \mathbf{G} remains necessarily finite, leading to a runaway to infinity of the coupling constants as updated by the gradient-descent algorithm: $K'_r = K_r - \epsilon G_r$ (with $\epsilon \ll 1$ the step variable in the numerical implementation of the gradient descent). In this case, the algorithm converges in practice when the minimal distance $|\mathbf{G}_\infty|^2 = \min_{LV} \sum_r \langle (f_r)_{LV} - \langle f_r \rangle_Q \rangle^2$ between the LV predictions and the classical data is attained numerically. This convergence criterion marks the fact that the variational search of the LV model has hit from the inside a facet of the polytope (Fig. 1C), defining a Bell inequality violated by the quantum data. The latter inequality stems from a simple rewriting of the condition $|\mathbf{G}_\infty|^2 > 0$, namely

$$\sum_r G_{r,\infty} \langle f_r \rangle_Q < \min_{LV} \sum_r G_{r,\infty} \langle f_r \rangle_{LV} = -B_c. \quad (8)$$

The minimization of the right-hand side of Eq. (8) – defining the classical bound B_c – is attained as the ground-state energy of the following effective Hamiltonian \mathcal{K} (not to be confused with \mathcal{H}):

$$\mathcal{K}(\boldsymbol{\sigma}) = \sum_r G_{r,\infty} f_r(\boldsymbol{\sigma}). \quad (9)$$

Interestingly, we observe that $\mathcal{K}(\boldsymbol{\sigma})$ is necessarily a frustrated Hamiltonian, namely a function whose minimum is not obtained by minimizing each term $G_{r,\infty} f_r(\boldsymbol{\sigma})$ individually. Indeed, in the absence of frustration, the quantum data has no chance of being strictly lower than the classical bound defined in Eq. (8).

Before demonstrating the practical use of our approach, we would like to point out its computational efficiency. Its strength relies fundamentally upon its data-driven nature. Indeed, instead of trying to reconstruct the whole local polytope (potentially producing a large number of unviolated Bell inequalities), our approach directly tests for the non-locality of a particular quantum data set – corresponding to what an experiment (actual or numerical) can achieve – and it delivers a Bell inequality violated by the available quantum data. Its main computational cost is imposed by the calculation of the statistical averages $\langle f_r(\boldsymbol{\sigma}) \rangle_{LV}$: such a calculation is generically efficient and scalable to arbitrary N by using classical Monte Carlo, unless the Ising Hamiltonian $\mathcal{H}(\boldsymbol{\sigma}; \mathbf{K})$ happens to be a spin-glass model – something which is categorically

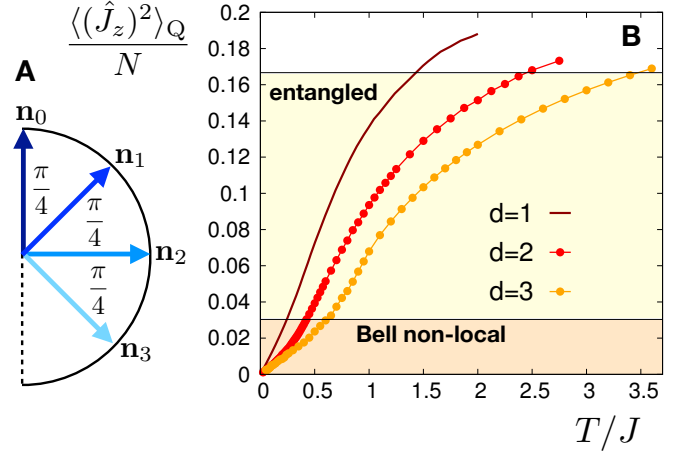


FIG. 2: Many-body Bell non-locality of quantum Heisenberg antiferromagnets. (A) Measurement basis ($k = 4$) providing the strongest violation of the Bell inequality in Eq. (10) by the low-temperature data of quantum Heisenberg antiferromagnets; (B) Normalized fluctuations of a collective spin component, $\langle (\hat{J}_z)^2 \rangle_Q / N$, in Heisenberg antiferromagnets on the linear chain ($d = 1$), the square lattice ($d = 2$) and the cubic lattice ($d = 3$). The data shown are obtained via the Bethe-Ansatz prediction [23] for $d = 1$, and by quantum Monte Carlo ($d = 2, 3$) on lattices of size 30^2 and 12^3 respectively – the thermodynamic limit values are essentially reached for these sizes. When the fluctuations become smaller than the classical bound β_4 (see text) they witness the appearance of Bell non-locality; in the figure we report as well the known bound for witnessing entanglement [24, 25].

avoided if the quantum data have elementary spatial symmetries, and if the local observables are not chosen randomly. Otherwise, the computational cost of calculating $\langle f_r(\boldsymbol{\sigma}) \rangle_{LV}$ for N degrees of freedom with a relative precision of ϵ scales as $\mathcal{O}(\text{poly}(N) \times \epsilon^{-2})$ – where the order of the polynomial in N is related to the quantum data of interest, and it is at most $\mathcal{O}(N^n)$ if the f_r 's are correlation functions involving up to n points. Further details of the implementation of the method are offered in the Supplementary Information (SI).

As explained above, our approach starts from a thoughtfully chosen set of quantum data: in the following we will illustrate it in three paradigmatic cases, in which the input quantum data are offered by the spin expectation values and 2-point correlation functions of 1) a Bell pair; 2) the quantum critical point of the $d = 2$ transverse-field Ising model; and 3) the low-energy states of the Heisenberg antiferromagnet on hyper-cubic lattices.

We first explain the conceptual significance of our approach in the paradigmatic case of a Bell pair ($|\uparrow_1 \downarrow_2\rangle - |\downarrow_1 \uparrow_2\rangle$)/ $\sqrt{2}$ of two $S = 1/2$ spins. In the case of a (2,2,2) scenario, choosing the measurement basis $\sigma_0^{(1)} = \sigma_x$, $\sigma_1^{(1)} = \sigma_y$; $\sigma_0^{(2)} = \cos \theta \sigma_x + \sin \theta \sigma_y$, $\sigma_1^{(2)} = \cos \theta \sigma_x - \sin \theta \sigma_y$, one obtains the following quantum data for the correlation functions, $\langle \sigma_0^{(1)} \sigma_0^{(2)} \rangle_Q = \langle \sigma_1^{(1)} \sigma_1^{(2)} \rangle_Q = -\cos \theta$, and $\langle \sigma_0^{(1)} \sigma_1^{(2)} \rangle_Q = -\langle \sigma_1^{(1)} \sigma_0^{(2)} \rangle_Q = -\sin \theta$. Choosing the optimal angle $\theta = \pi/4$ leads to correlation functions which take

the common absolute value $1/\sqrt{2}$, but realize a fully frustrated correlation loop (three negative correlations and a positive one – see Fig. 1D). When trying to reproduce this correlation pattern with the equilibrium state of an Ising model $\mathcal{H} = -\sum_{a,b \in \{0,1\}} K_{ab} \sigma_a^{(1)} \sigma_b^{(2)}$, one can easily realize that the optimal choice is to take $K_{ab} = \beta J_{ab}$ with $\beta \rightarrow \infty$ (restricting the phase space to the ground state manifold of the Hamiltonian) and $J_{00} = J_{11} = J_{01} = -J_{10}$, defining a fully frustrated square (3 antiferromagnetic couplings and a ferromagnetic one), such that $\langle \sigma_0^{(1)} \sigma_0^{(2)} \rangle_{LV} = \langle \sigma_1^{(1)} \sigma_1^{(2)} \rangle_{LV} = \langle \sigma_0^{(1)} \sigma_1^{(2)} \rangle_{LV} = -\langle \sigma_1^{(1)} \sigma_0^{(2)} \rangle_{LV} = -1/4$ (since \mathcal{H} has 8 degenerate ground states, in which there is always one correlation function out of 4 with the wrong sign). As a consequence, one obtains for the gradient vector the components $G_{00} = G_{11} = G_{01} = -G_{10} = (2\sqrt{2} - 1)/4$ defining an effective Hamiltonian $\tilde{\mathcal{H}}$ which has the same form as \mathcal{H} , and which reconstructs the celebrated Clauser-Horne-Shimony-Holt (CHSH) inequality [26] $\langle \sigma_0^{(1)} \sigma_0^{(2)} + \sigma_1^{(1)} \sigma_1^{(2)} + \sigma_0^{(1)} \sigma_1^{(2)} - \sigma_0^{(1)} \sigma_1^{(2)} \rangle_{LV} \geq -B_c = -2$ (while the quantum data achieve the value $-2\sqrt{2}$).

Moving on to many-body systems, we consider the $2d$ transverse-field Ising model at its quantum-critical (QC) point. Here, the quantum data consist of the net magnetization and pair correlation functions. In the SI we show that our approach reconstructs a permutationally-invariant Bell inequality violated by the quantum data. The relevant inequality, first identified in Ref. [17], is violated by strongly squeezed states [27–29], and squeezing is also a property of the QC point in question [30]. Yet our approach allows us to make a stronger statement, namely that– given the $(N, 2, 2)$ scheme with measurement bases suggested by Ref. [27] – a symmetric Bell inequality is the one maximally violated by quantum data that are not at all symmetric (unlike those produced in the experiments of Refs. [27, 28]), because of the spatial decay of correlations functions at criticality.

We conclude our article by focusing on the equilibrium states of a paradigmatic quantum spin-lattice model, namely the quantum Heisenberg antiferromagnet (QHAF) with Hamiltonian $\hat{\mathcal{H}} = J \sum_{\langle ij \rangle} \hat{S}^{(i)} \cdot \hat{S}^{(j)}$, where $\hat{S}^{(i)}$ are quantum $S = 1/2$ operators, and the sum runs over pairs of nearest neighbors on a hypercubic lattice with an even number of sites. The ground state of this model realizes a global singlet, namely a many-body generalization of the Bell pair considered above. We focus on a $(N, k, 2)$ scenario, with $k \geq 3$ measurements per spin along axes \mathbf{n}_a ($a = 0, 1, \dots, k-1$), and we consider a uniform measurement strategy in which the axes are coplanar and form an angle $a\pi/k$ with a given reference axis (this turns out to be optimal) – see Fig. 2A. Feeding our algorithm with the two-point correlation function of the $2d$ QHAF as quantum data, we discover that the latter violate the following symmetric Bell inequality

$$\langle \mathcal{B} \rangle_{LV} = \sum_{a=0}^{k-1} \mathcal{S}_{aa} + \sum_{a=0}^{k-2} \mathcal{S}_{a,a+1} - \mathcal{S}_{k-1,0} \geq -B_c = -2N(k-1) \quad (10)$$

for all $k \geq 3$, where $\mathcal{S}_{ab} = \sum_{i \neq j} \langle \sigma_a^{(i)} \sigma_b^{(j)} \rangle_{LV}$. This inequality

– which is proved rigorously in the SI – turns out to be a many-body extension of the Pearle-Braunstein-Caves inequality [31, 32] proposed for non-locality detection in 2-spin states in a more robust fashion than what is achieved with the CHSH inequality. Indeed, using $k \geq 3$ inputs per site requires the LV model to reproduce a larger set of quantum data, hence the increased robustness [32]. Similarly to the above-cited example of the QC point of the $2d$ quantum Ising model, it is remarkable to notice that quantum data with spatial structure – such as the correlation function of the $2d$ QHAF – are found to maximally violate a Bell inequality in which the spatial structure is washed out by the symmetrization procedure.

To see explicitly that the ground state of the QHAF violates the inequality of Eq. (10), we make use of the $SU(2)$ invariance to rewrite the Bell operator $\hat{\mathcal{B}}$ in the form (see the SI):

$$\hat{\mathcal{B}} = 4k[1 + \cos(\pi/k)]\hat{J}_z^2 - Nk \cos(\pi/k) - Nk \quad (11)$$

where $\hat{J}_z = \sum_i \hat{S}_z^{(i)}$ is the collective spin along z . Therefore the classical bound $-B_c$ is violated by the quantum data whenever

$$\frac{\langle \hat{J}_z^2 \rangle_Q}{N} < \beta_k = \frac{2 - k[1 - \cos(\pi/k)]}{4k[1 + \cos(\pi/k)]} \quad (12)$$

where the largest value of the right-hand side is found for $k = 4$, and it reads $\beta_4 = 1/(16 + 12\sqrt{2}) = 0.030330\dots$. Eq. (12) states that a sufficiently low value of the variance of one collective spin component (below the β_4 bound) is a witness [27] of Bell non-locality (“witness” because, in order to derive it, we explicitly used the spin algebra as well as the hypothesis of $SU(2)$ invariance of the state). The ground state of all Heisenberg antiferromagnets with even N (regardless of the geometry of the underlying lattice) are total spin singlets (such that $\langle \hat{J}_z^2 \rangle_Q = 0$), and hence they satisfy the above criterion and violate the Bell inequality of Eq. (10). Moreover, in the SI we show that the quantum violation of the inequality Eq. (10) offered by total spin singlets, $\langle \hat{\mathcal{B}} \rangle_Q = -Nk[1 + \cos(\pi/k)]$, is the maximal violation authorized by quantum mechanics (namely, regardless of the dimension of the Hilbert space of the system, its quantum state, and the chosen measurements). Fig. 2B shows that the condition Eq. (12) is also met by thermal equilibrium states of the QHAF in $d = 1, 2$ and 3 up to very sizable temperatures (the higher the larger d is, as non-locality is clearly protected by the strength of antiferromagnetic correlations). The condition of Eq. (12) is to be contrasted with the much looser one, $\langle \hat{J}_z^2 \rangle_Q/N < 1/6$ required to witness entanglement between the individual spins [24, 25] – namely to exclude the possibility of writing the state of the system as $\rho = \sum_s p_s \otimes_i \rho_s^{(i)}$, where $\rho_s^{(i)}$ are mixed states of individual spins. This reflects the fact that, for mixed states, Bell non-locality is a much stronger form of quantum correlations than entanglement. Moreover the fundamental connection between the collective spin variance and the spin susceptibility at thermal equilibrium $\chi_z = \langle \hat{J}_z^2 \rangle_Q / (k_B T N)$ (where T is the temperature) makes the above witness of non-locality experimentally accessible to magnetometry experiments on quantum magnets at realistic temperatures.

In conclusion, we have demonstrated a variational approach which can assess whether an arbitrary set of quantum data, coming from scalable quantum many-body systems, exhibits quantum non-locality; and which reconstructs the Bell inequality maximally violated by a linear combination of the data at hand. The computational cost of the algorithm is polynomial in system size whenever the quantum data are not obtained from quantum systems governed by random Hamiltonians, and are not obtained by using a random measurement basis for each degree of freedom – and it may still remain polynomial even if the above conditions are not met. Therefore, our approach opens the door to scalable and systematic certification of entanglement in synthetic quantum matter (quantum simulators [33, 34], quantum processors [35, 36]). When the violated Bell inequalities have a symmetric structure under the exchange of degrees of freedom (as in the case of the Heisenberg antiferromagnets reported in this work), a witness of Bell non-locality can be formulated by using collective ob-

servables only [27], and the latter is therefore accessible in the broader context of quantum materials in condensed matter physics.

Acknowledgments

We warmly thank A. Acín, A. Aloy, A. Aspect, F. Baccari, C. Branciard, M. Lewenstein, P. Ronceray, L. Tagliacozzo, and J. Tura for insightful discussions and encouragement. This work is supported by ANR (“EELS” project), QuantERA (“MAQS” project), the Spanish MINECO (Severo Ochoa SEV-2015-0522), the fundacio Mir-Puig and Cellex through an ICFO-MPQ postdoctoral fellowship, and the Generalitat de Catalunya (SGR 1381, QuantumCAT and CERCA Programme).

-
- [1] R. Horodecki, P. Horodecki, M. Horodecki, and K. Horodecki, *Rev. Mod. Phys.* **81**, 865 (2009), URL <https://link.aps.org/doi/10.1103/RevModPhys.81.865>.
 - [2] R. Uola, A. C. S. Costa, H. Chau Nguyen, and O. Gühne, *arXiv e-prints arXiv:1903.06663* (2019), 1903.06663.
 - [3] M. D. Reid, P. D. Drummond, W. P. Bowen, E. G. Cavalcanti, P. K. Lam, H. A. Bachor, U. L. Andersen, and G. Leuchs, *Rev. Mod. Phys.* **81**, 1727 (2009), URL <https://link.aps.org/doi/10.1103/RevModPhys.81.1727>.
 - [4] N. Brunner, D. Cavalcanti, S. Pironio, V. Scarani, and S. Wehner, *Rev. Mod. Phys.* **86**, 419 (2014), URL <https://link.aps.org/doi/10.1103/RevModPhys.86.419>.
 - [5] V. Scarani, *Bell nonlocality* (Oxford University Press, 2019).
 - [6] J. P. Dehollain, S. Simmons, J. T. Muhonen, R. Kalra, A. Laucht, F. Hudson, K. M. Itoh, D. N. Jamieson, J. C. McCallum, A. S. Dzurak, et al., *Nature Nanotechnology* **11**, 242 (2016), ISSN 1748-3395, URL <https://doi.org/10.1038/nnano.2015.262>.
 - [7] A. Aspect, P. Grangier, and G. Roger, *Phys. Rev. Lett.* **49**, 91 (1982), URL <https://link.aps.org/doi/10.1103/PhysRevLett.49.91>.
 - [8] W. Zurek, *Physics Today* **44**, 36 (1991).
 - [9] M. Schlosshauer, *Physics Reports* **831**, 1 (2019), ISSN 0370-1573, quantum decoherence, URL <http://www.sciencedirect.com/science/article/pii/S0370157319303084>.
 - [10] A. Acín, I. Bloch, H. Buhrman, T. Calarco, C. Eichler, J. Eisert, D. Esteve, N. Gisin, S. J. Glaser, F. Jelezko, et al., *New Journal of Physics* **20**, 080201 (2018), URL <https://doi.org/10.1088%2F1367-2630%2Faad1ea>.
 - [11] J. S. Bell, *Physics* **1**, 195 (1964).
 - [12] A. Fine, *Phys. Rev. Lett.* **48**, 291 (1982), URL <https://link.aps.org/doi/10.1103/PhysRevLett.48.291>.
 - [13] N. D. Mermin, *Phys. Rev. Lett.* **65**, 1838 (1990), URL <https://link.aps.org/doi/10.1103/PhysRevLett.65.1838>.
 - [14] O. Gühne, G. Tóth, P. Hyllus, and H. J. Briegel, *Phys. Rev. Lett.* **95**, 120405 (2005), URL <https://link.aps.org/doi/10.1103/PhysRevLett.95.120405>.
 - [15] J. Tura, G. De las Cuevas, R. Augusiak, M. Lewenstein, A. Acín, and J. Cirac, *Phys. Rev. X* **7**, 021005 (2017), URL <https://link.aps.org/doi/10.1103/PhysRevX.7.021005>.
 - [16] B. P. Lanyon, M. Zwerger, P. Jurcevic, C. Hempel, W. Dür, H. J. Briegel, R. Blatt, and C. F. Roos, *Phys. Rev. Lett.* **112**, 100403 (2014), URL <https://link.aps.org/doi/10.1103/PhysRevLett.112.100403>.
 - [17] J. Tura, R. Augusiak, A. B. Sainz, T. Vértesi, M. Lewenstein, and A. Acín, *Science* **344**, 1256 (2014), ISSN 0036-8075, URL <http://science.sciencemag.org/content/344/6189/1256>.
 - [18] F. Baccari, D. Cavalcanti, P. Wittek, and A. Acín, *Phys. Rev. X* **7**, 021042 (2017), URL <https://link.aps.org/doi/10.1103/PhysRevX.7.021042>.
 - [19] E. T. Jaynes, *Phys. Rev.* **106**, 620 (1957), URL <https://link.aps.org/doi/10.1103/PhysRev.106.620>.
 - [20] Y. Tikochinsky, N. Z. Tishby, and R. D. Levine, *Phys. Rev. A* **30**, 2638 (1984), URL <https://link.aps.org/doi/10.1103/PhysRevA.30.2638>.
 - [21] H. C. Nguyen, R. Zecchina, and J. Berg, *Advances in Physics* **66**, 197 (2017), <https://doi.org/10.1080/00018732.2017.1341604>, URL <https://doi.org/10.1080/00018732.2017.1341604>.
 - [22] S. Boyd, S. Boyd, and L. Vandenberghe, *Convex Optimization* (Cambridge University Press, 2004).
 - [23] S. Eggert, I. Affleck, and M. Takahashi, *Phys. Rev. Lett.* **73**, 332 (1994), URL <https://link.aps.org/doi/10.1103/PhysRevLett.73.332>.
 - [24] G. Tóth, *Phys. Rev. A* **69**, 052327 (2004), URL <https://link.aps.org/doi/10.1103/PhysRevA.69.052327>.
 - [25] M. Wieśniak, V. Vedral, and Č. Brukner, *New Journal of Physics* **7**, 258 (2005), URL <https://doi.org/10.1088%2F1367-2630%2F7%2F1%2F258>.
 - [26] J. F. Clauser, M. A. Horne, A. Shimony, and R. A. Holt, *Phys. Rev. Lett.* **23**, 880 (1969), URL <https://link.aps.org/doi/10.1103/PhysRevLett.23.880>.

- [27] R. Schmied, J.-D. Bancal, B. Allard, M. Fadel, V. Scarani, P. Treutlein, and N. Sangouard, *Science* **352**, 441 (2016), ISSN 0036-8075, 1095-9203, URL <http://science.sciencemag.org/content/352/6284/441>.
- [28] N. J. Engelsen, R. Krishnakumar, O. Hosten, and M. A. Kasevich, *Phys. Rev. Lett.* **118**, 140401 (2017), URL <https://link.aps.org/doi/10.1103/PhysRevLett.118.140401>.
- [29] A. Piga, A. Aloy, M. Lewenstein, and I. Frérot, *Phys. Rev. Lett.* **123**, 170604 (2019), URL <https://link.aps.org/doi/10.1103/PhysRevLett.123.170604>.
- [30] I. Frérot and T. Roscilde, *Phys. Rev. Lett.* **121**, 020402 (2018), URL <https://link.aps.org/doi/10.1103/PhysRevLett.121.020402>.
- [31] P. M. Pearle, *Phys. Rev. D* **2**, 1418 (1970), URL <https://link.aps.org/doi/10.1103/PhysRevD.2.1418>.
- [32] S. L. Braunstein and C. M. Caves, *Annals of Physics* **202**, 22 (1990), ISSN 0003-4916, URL <http://www.sciencedirect.com/science/article/pii/000349169090339P>.
- [33] I. M. Georgescu, S. Ashhab, and F. Nori, *Rev. Mod. Phys.* **86**, 153 (2014), URL <https://link.aps.org/doi/10.1103/RevModPhys.86.153>.
- [34] E. Altman, K. R. Brown, G. Carleo, L. D. Carr, E. Demler, C. Chin, B. DeMarco, S. E. Economou, M. A. Eriksson, K.-M. C. Fu, et al., *arXiv e-prints arXiv:1912.06938* (2019), 1912.06938.
- [35] G. Wendin, *Reports on Progress in Physics* **80**, 106001 (2017), URL <https://doi.org/10.1088%2F1361-6633%2Faa7e1a>.
- [36] C. D. Bruzewicz, J. Chiaverini, R. McConnell, and J. M. Sage, *Applied Physics Reviews* **6**, 021314 (2019), <https://doi.org/10.1063/1.5088164>, URL <https://doi.org/10.1063/1.5088164>.
- [37] F. Barahona, *Journal of Physics A: Mathematical and General* **15**, 3241 (1982), URL <https://doi.org/10.1088%2F0305-4470%2F15%2F10%2F028>.
- [38] C. P. Bachas, *Journal of Physics A: Mathematical and General* **17**, L709 (1984), URL <https://doi.org/10.1088%2F0305-4470%2F17%2F13%2F006>.
- [39] H. W. J. Blöte and Y. Deng, *Phys. Rev. E* **66**, 066110 (2002), URL <https://link.aps.org/doi/10.1103/PhysRevE.66.066110>.

SUPPLEMENTARY INFORMATION

Detecting many-body Bell nonlocality by solving Ising models

Irénée Frérot^{1,2} and Tommaso Roscilde³

¹ ICFO-Institut de Ciències Fòniques, The Barcelona Institute of Science and Technology, Av. Carl Friedrich Gauss 3, 08860 Barcelona, Spain

² Max-Planck-Institut für Quantenoptik, D-85748 Garching, Germany

³ Laboratoire de Physique, CNRS UMR 5672, Ecole Normale Supérieure de Lyon, Université de Lyon, 46 Allée d'Italie, Lyon, F-69364, France

I. IMPLEMENTATION OF THE VARIATIONAL APPROACH

In this section we describe the practical implementation of the algorithm for the search of Bell inequalities as starting from a set of thoughtfully chosen quantum data. More elements about the choice of the quantum data – specifically for what concerns the choice of the measurement basis – will be discussed in Secs. II and IV.

A. Monte Carlo treatment of the local-variable theory

The goal of the algorithm is to reproduce the quantum data using the equilibrium behavior of a classical statistical physics model describing Ising variables (for $p = 2$) on a lattice, or more generally with variables admitting an arbitrary number p of values. As discussed in the main text, this represent an efficient strategy to produce a local-variable (LV) theory for the data of interest. In the following we will concentrate for concreteness on the (N, k, p) scenario with $p = 2$, but the discussion can be readily generalized to arbitrary p 's. The quantum data generically consists of average values of functions $f_r(\sigma)$ of the measurement outputs $\{\sigma_a^{(i)}\}$ ($a = 0, \dots, k-1$, $i = 1, \dots, N$) on the quantum degrees of freedom, which we shall denote as qubits in the following (since $p = 2$); such functions are then used to build the Hamiltonian of the classical model in the form:

$$\mathcal{H}(\sigma; \mathbf{K}) = - \sum_r K_r f_r(\sigma). \quad (13)$$

Throughout the work presented here, we have specialized our attention to single-site expectation values and two-point correlation functions, namely $\{f_r(\sigma)\} = \{\sigma_a^{(i)}\}, \{\sigma_a^{(i)} \sigma_b^{(j \neq i)}\}$; but obviously the whole treatment generalizes to arbitrary correlation functions.

The core of the variational algorithm is the calculation of the statistical averages representing the predictions of the LV theory

$$\langle f_r(\sigma) \rangle_{LV} = \frac{1}{\mathcal{Z}(\mathbf{K})} \sum_{\sigma} f_r(\sigma) e^{-\mathcal{H}(\sigma; \mathbf{K})} \quad (14)$$

and building up the gradient of the cost function (Eq. 5 of the main text)

$$G_r = \langle f_r(\boldsymbol{\sigma}) \rangle_{LV} - f_r(\boldsymbol{\sigma})_Q \quad (15)$$

which is then used to update the coupling constants within a gradient-descent algorithm. In our calculations we have actually implemented Nesterov's accelerated gradient descent, which offers a dramatic speed-up, often reducing the cost function exponentially in the number of iterations – yet with the mild drawback that the cost function is not necessarily decreasing at each step of the algorithm.

The effective Hamiltonian of Eq. (13) has a structure involving generically long-range couplings and external fields (see below); a general, fully scalable strategy to calculate efficiently the statistical averages of Eq. (14) is then to use a standard Monte Carlo (MC) algorithm with single spin-flip Metropolis updates. Defining a single MC step as $\mathcal{O}(N)$ spin-flip attempts, the statistical error $\text{Err}(\langle f_r(\boldsymbol{\sigma}) \rangle_{LV})$ on the LV averages $\langle f_r(\boldsymbol{\sigma}) \rangle_{LV}$ scales as $c N_{MC}^{-1/2}$ where N_{MC} is the number of MC steps and c is a size-independent prefactor.

In a practical calculation aimed at optimizing the LV theory, one in fact needs to have a good relative precision not on the LV observables as such, but rather on the gradient as in Eq. (15) – for instance one may require that

$$\frac{\text{Err}(|\mathbf{G}|^2)}{|\mathbf{G}|^2} = \frac{\sum_{r=1}^R 2 \text{Err}(\langle f_r(\boldsymbol{\sigma}) \rangle_{LV}) |G_r|}{\sum_r |G_r|^2} \leq \eta \quad (16)$$

for a given tolerance η , in order for the gradient to be calculated with sufficient precision so as to offer practical guidance in the optimization. For the time being we have neglected the uncertainty on the quantum data, assuming that it is much smaller than the statistical uncertainty on the LV averages. This means that the number of Monte Carlo steps scales in practice as $N_{MC} \sim (\eta |\mathbf{G}|^2)^{-2}$, namely the cost of the MC simulation grows as the distance $|\mathbf{G}|$ between the LV predictions and the quantum data decreases.

The above result on the scaling of the MC steps with the gradient norm would naively imply that, if the LV theory succeeds to reproduce the quantum data ($|\mathbf{G}| \rightarrow 0$), then the cost of the computation of the LV averages would diverge. This is in fact not the case, when taking into account an inevitable finite precision on the quantum data, namely that $\text{Err}(\langle f_r(\boldsymbol{\sigma}) \rangle_Q) > 0$. In that case, convergence of the LV theory occurs *within* the precision of the quantum data, and this imposes a minimal error on the LV averages of the same order of magnitude. Hence the maximum number of MC steps necessary to assess convergence of the LV theory to the quantum data is of the order $N_{MC} \sim \max_r [\text{Err}(\langle f_r(\boldsymbol{\sigma}) \rangle_Q)^{-2}]$.

Otherwise, if the LV theory fails to reproduce the quantum data, the gradient norm saturates to a finite minimum $|\mathbf{G}_\infty|$; and the number of MC steps necessary to reach this conclusion saturates to $N_{MC} \sim (\eta |\mathbf{G}_\infty|^2)^{-2}$. In our calculations we have found that a tolerance $\eta = 0.05$ provides a manageable cost (with $N_{MC} \sim 10^6 \div 10^7$ for the systems we considered) while providing a sufficient accuracy on the gradient for the optimization to be effective.

B. Effective local-variable Hamiltonian structured by the quantum data

The structure of the quantum data $\langle f_r(\boldsymbol{\sigma}) \rangle_Q$ that we aim at reproducing fundamentally consists of two ingredients: 1) the geometry of the observables collected on the qubits (namely, what correlation functions among which qubits have been measured, etc.) ; and 2) the spatial structure of the measured observables (namely, what values the correlation functions actually take). Such properties of the quantum data fundamentally dictate the structure and physical properties of the effective Hamiltonian to be treated. In the following we shall make some conservative assumptions on both aspects of the structure of quantum data, which guarantee the success of our approach; and we shall briefly discuss the possible lifting of such assumptions.

Geometry of the observables. We shall assume some basic regularity in the choice of observables used to probe the quantum system – namely the fact that, once the local measurement basis has been chosen (not necessarily in the same way for all qubits), then the same amount of information is acquired on each qubit and on its correlations to the other qubits. Arranging the qubits on a regular lattice with site index i , we shall imagine for instance that the quantum data contain the average value of all the measurements on individual qubits $\langle \sigma_a^{(i)} \rangle_Q$ for *all* a and i ; and all the correlation functions among local measurements on qubits lying within a given mutual distance D , namely $\langle \sigma_a^{(i)} \sigma_b^{(j)} \rangle_Q$ for *all* a, b and for *all* $i \neq j$ such that $|i - j| \leq D$, etc. Such a choice endows then the classical model with a regular lattice structure, with local field terms $-K_a^{(i)} \sigma_a^{(i)}$ coupling to each local variable, and with interaction terms $-K_{ab}^{(ij)} \sigma_a^{(i)} \sigma_b^{(j)}$ among all local variables within a given mutual distance. Non-locality is best detected when using as much information as possible on the quantum state; in particular, given access to the n -point correlation function, it is sensible to use the information on its entire structure, containing $\mathcal{O}(N^n)$ terms. Under this assumption, the LV effective Hamiltonian Eq. (13) aimed at reproducing the full n -point correlation function contains a number $\mathcal{O}(N^n)$ of terms, implying a computational cost scaling in the same way with N for the MC evaluation of the LV averages. In all the calculations presented in this work we have restricted our attention to the case $n = 2$.

Spatial structure of the measured observables. Once the geometry of the coupling constants $\{K_r\}$ has been fixed by the geometry of the observables contained in the quantum data, the values of such constants are adjusted in order to best reproduce the quantum data with an LV theory. Despite the regularity of the lattice into which the qubits are arranged, a preparation of their quantum state using random protocols (the equilibrium or non-equilibrium physics of random quantum Hamiltonians; random sequences of gates, etc.) will lead to quantum data with little or no structure, which may in turn require random couplings K_r in the LV theory that aims at reproducing them. Avoiding randomness is a rather safe assumption in order to guarantee convergence for the Monte Carlo calculations of the LV averages (see below for further

discussion). We can state that our approach is fully scalable – namely capable of testing non-locality for the state of N qubits in a time scaling polynomially with N – when considering quantum data endowed with basic symmetries (e.g. translational invariance on a lattice with periodic boundary conditions, reflection symmetry on a regular lattice with open boundary conditions, etc.). Throughout this work we have used quantum data which come from the equilibrium physics of translationally invariant models (defined on regular lattices with periodic boundary conditions), which is a rather convenient situation as it allows one to reduce the number of independent coupling constants by a factor of N .

Relaxing some of the above assumptions (on the regularity on the choice of observables building up the quantum data, and on the symmetries of the quantum data) may potentially expose the variational search of the LV theory to a much higher computational cost, which is required in the case in which the effective Hamiltonian Eq. (13) is a model of an Ising spin glass – namely a model containing frustration and randomness. While frustration is a generic ingredient of LV theories aiming at reproducing a set of quantum data, randomness is precisely avoided by the above assumptions. Some instances of Ising spin glasses are known to be computationally hard [37, 38], namely the calculation of their equilibrium properties is faced with the existence of a large number of metastable states, so that the convergence of MC simulations towards the correct Boltzmann averages (Eq. (14)) is only guaranteed in a time scaling exponentially with N . Nonetheless it is very difficult to assess a priori the computational cost in the calculation of statistical averages for the frustrated and disordered Ising models that correspond to LV theories aiming at reproducing a particular set of quantum data with randomness. We take the above assumptions on the structure of quantum data as being *sufficient* (namely conservative) conditions for the convergence of our approach in a time scaling polynomially with system size. At the same time, one may reasonably expect that a moderate amount of randomness in the quantum data (either stemming from a random choice of the observables, or from randomness in the quantum state) can be tolerated without generating an exponential cost for the convergence of our approach.

II. DETECTING NON-LOCALITY OF THE 2d TRANSVERSE-FIELD ISING MODEL AT THE QUANTUM CRITICAL POINT

In this section we shall focus on the quantum critical point of the 2d quantum Ising model; and we shall describe how our algorithm recovers the many-body Bell inequality originally discovered in Ref. [17] as the Bell inequality which is most strongly violated by quantum data consisting of one-site and two-site expectation values in a $(N, 2, 2)$ scenario.

A. Frustration of the LV theories from squeezing and polarization

The Hamiltonian of the 2d quantum Ising model reads

$$\hat{\mathcal{H}} = -J \sum_{\langle ij \rangle} \hat{S}_z^{(i)} \hat{S}_z^{(j)} - \Gamma \sum_i \hat{S}_x^{(i)} \quad (17)$$

where $\langle ij \rangle$ represents a pair of nearest neighbors on a $L \times L$ square lattice with periodic boundary conditions, and $\hat{S}_\alpha^{(i)}$ ($\alpha = x, y, z$) are $S = 1/2$ spin operators. For definiteness, in the following we shall consider ferromagnetic couplings ($J > 0$). The above model exhibits a quantum phase transition when the transverse field hits the critical value $\Gamma_c = 1.52219(1)J$ [39]: the critical point is accompanied with squeezing of the fluctuations of the y component of the collective spin, $\hat{J}_y = \sum_i \hat{S}_y^{(i)}$ [30], namely with the property that the spin-spin correlation for the y component of the spins is negative, $C_{yy}^{(ij)} = \langle \hat{S}_y^{(i)} \hat{S}_y^{(j)} \rangle < 0 \ \forall i \neq j$, while the correlation functions C_{xx} and C_{zz} for the x and z spin components are clearly positive. The appearance of sufficiently strong squeezing leads to Bell non-locality in a $(N, 2, 2)$ scenario, as shown experimentally in Ref. [27] for the squeezed state of an atomic spin ensemble; in the latter reference the following uniform measurement strategy was suggested

$$\hat{\sigma}_0 = \cos \theta \hat{\sigma}_x + \sin \theta \hat{\sigma}_y \quad \hat{\sigma}_1 = \cos \theta \hat{\sigma}_x - \sin \theta \hat{\sigma}_y \quad (18)$$

where $\hat{\sigma}_{x,y}$ are Pauli matrices. Such a strategy was used to build a Bell non-locality witness – namely an inequality on observables derived from the Bell inequality of Ref. [17] upon assuming the spin algebra – based on the squeezing parameter $\xi^2 = N \text{Var}(\hat{J}_y) / \langle \hat{J}_x \rangle^2$ and on the polarization $m_x = \langle \hat{J}_x \rangle / N = \langle \sum_i \hat{S}_x^{(i)} \rangle / N$.

As input to the Bell test we shall use the quantum data composed of the average local observables and of their two-point correlation functions, namely

$$\begin{aligned} \langle \sigma_0^{(i)} \rangle_Q &= \langle \sigma_1^{(i)} \rangle_Q = 2 \cos \theta m_x \\ \langle \sigma_0^{(i)} \sigma_0^{(j)} \rangle_Q &= \langle \sigma_1^{(i)} \sigma_1^{(j)} \rangle_Q = 4 \cos^2 \theta C_{xx}^{(ij)} + 4 \sin^2 \theta C_{yy}^{(ij)} \\ \langle \sigma_0^{(i)} \sigma_1^{(j)} \rangle_Q &= 4 \cos^2 \theta C_{xy}^{(ij)} - 4 \sin^2 \theta C_{yy}^{(ij)} \end{aligned} \quad (19)$$

where we have used the fact that $\langle \hat{S}_x^{(i)} \hat{S}_y^{(j)} \rangle = 0$. From the point of view of our variational approach, the Bell test consists in actively building an LV theory in the form of an Ising model with two Ising variables ($\sigma_0^{(i)}$ and $\sigma_1^{(i)}$) per physical lattice site – see Fig. 3(A). In practice the LV theory aims at reproducing the quantum data via the equilibrium thermodynamics of a classical Ising model in an external field, with an effective Hamiltonian directly reflecting the content of the quantum data, namely containing all possible one-spin and

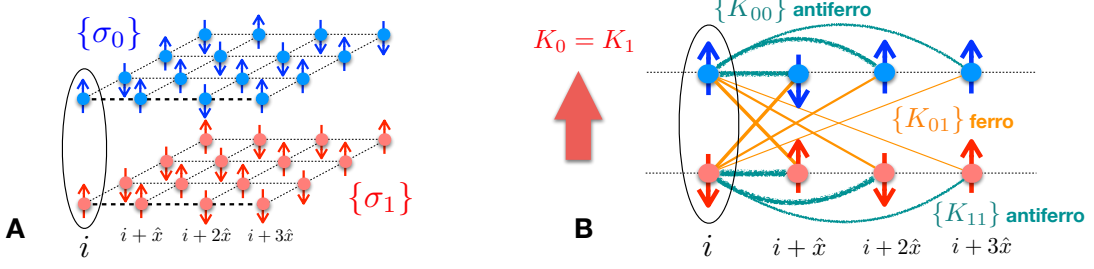


FIG. 3: Building the LV theory for the $2d$ quantum Ising model at its quantum critical point. A: in the $(N, 2, 2)$ scheme each lattice has attached two spin variables $\sigma_0^{(i)}$ and $\sigma_1^{(i)}$, so that the corresponding LV theory corresponds to an Ising model on a bilayer. B: sketch of the couplings emanating from a lattice i along the x direction of the lattice; in order to account for the fact that $\langle \sigma_0^{(i)} \sigma_1^{(j)} \rangle_Q > \langle \sigma_0^{(i)} \sigma_0^{(j)} \rangle_Q = \langle \sigma_1^{(i)} \sigma_1^{(j)} \rangle_Q$ in the presence of a strong polarization induced by the field $K_0 = K_1$, the LV theory develops frustration for the K_{00} and K_{11} couplings, as they are antiferromagnetic ($K_{00}^{(ij)} = K_{11}^{(ij)} < 0, \forall i \neq j$) and long-ranged, while the K_{01} couplings are ferromagnetic and therefore unfrustrated ($K_{01}^{(ij)} > 0, \forall i \neq j$).

two-spin terms

$$\begin{aligned} \mathcal{H}(\sigma; \mathbf{K}) = & - \sum_i \left(K_0 \sigma_0^{(i)} + K_1 \sigma_1^{(i)} \right) \\ & - \sum_{i < j} \left[K_{00}^{|i-j|} \sigma_0^{(i)} \sigma_0^{(j)} + K_{11}^{|i-j|} \sigma_1^{(i)} \sigma_1^{(j)} \right. \\ & \left. + K_{01}^{|i-j|} \left(\sigma_0^{(i)} \sigma_1^{(j)} + \sigma_1^{(i)} \sigma_0^{(j)} \right) \right] \quad (20) \end{aligned}$$

Here the translational invariance of the coupling constants (uniform fields K_0 and K_1 , and K_{ab} couplings uniquely dependent on the distance $|i - j|$ between sites) descends from the same invariance in the quantum data.

A simple argument suggests that the terms in the above effective Hamiltonian must be competing in energy (and therefore frustrated) in order to reproduce the quantum data of Eq. (19). Indeed the quantum data impose on the classical Ising variables in the Hamiltonian (20) seemingly contradictory requirements: the local variables should exhibit the same polarization $\langle \sigma_0 \rangle = \langle \sigma_1 \rangle$ and the same *intra*-variable correlation functions $\langle \sigma_0^{(i)} \sigma_0^{(j)} \rangle = \langle \sigma_1^{(i)} \sigma_1^{(j)} \rangle$; yet, because of the negativity of the C_{yy} correlator, the quantum data exhibit different *inter*-variable correlation functions, namely $\langle \sigma_0^{(i)} \sigma_1^{(j)} \rangle > \langle \sigma_0^{(i)} \sigma_0^{(j)} \rangle > 0$. Such a situation could be in principle stabilized at finite temperature by simply taking different coupling constants $K_{01} > K_{00} = K_{11}$, so that thermal effects have different impact on the inter- vs. intra-variable correlations. Yet, if the polarization of the variables ($2 \cos \theta m_x$) is sufficiently strong, such thermal effects should be significantly suppressed by the fields K_0 and K_1 , and the difference between intra- and inter-variable correlations is not justified.

The way out of this contradiction is that the coupling constants K_{00}, K_{11} have opposite signs with respect to the couplings K_{01} ; in particular, given the hierarchy of correlations, the K_{01} couplings should be taken as ferromagnetic (namely positive) so as to stabilize the positive dominant $\langle \sigma_0 \sigma_1 \rangle$ correlations; while the K_{00} and K_{11} couplings should be taken as anti-ferromagnetic (negative), so as to suppress the $\langle \sigma_0 \sigma_0 \rangle$ and $\langle \sigma_1 \sigma_1 \rangle$ correlations. In particular the long-range nature

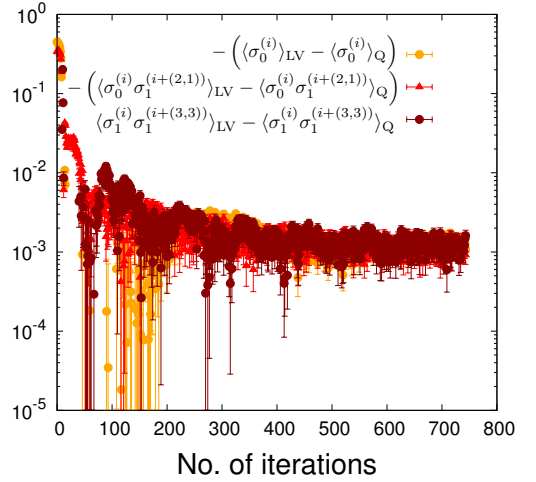


FIG. 4: Convergence of the gradient components of the cost function, $G_r = \langle f_r \rangle_{LV} - \langle f_r \rangle_Q$, to their asymptotic value, corresponding to the minimum of the cost function. The data shown correspond to three representative components for the distance to the quantum data of the $2d$ quantum Ising model on a 6×6 lattice at its quantum critical point, and for the angle $\theta = 0.3\pi$.

of the latter antiferromagnetic couplings leads to frustration – see Fig. 3(B). Such a frustrated configuration of couplings is indeed the one corresponding to the unique global minimum of the cost function optimized in order for the LV theory to best reproduce the quantum data.

B. Convergence of the algorithm and emergence of the Bell inequality

Here we shall illustrate how the variational algorithm indicates the failure of the LV theory to reproduce the quantum data, and how it unveils the Bell inequality maximally violated by the quantum data.

Fig. 4 shows the evolution of a few representative components of the cost function gradient (namely the distance vector

between the LV predictions and the quantum data) as calculated for the $2d$ quantum Ising model on a 6×6 lattice at its quantum critical point. The evolution follows an accelerated gradient descent with increment $\epsilon = 10^{-2}$. We observe that all the gradient components saturate to a finite asymptotic value, clearly manifesting a runaway behavior of the minimum search for the cost function (see main text). Moreover, and most significantly, all gradient components seemingly converge to the *same* absolute value, with a specific sign pattern. Such a sign pattern reconstructs a Bell inequality of the following form

$$\begin{aligned} & - \sum_i \left(\sigma_0^{(i)} + \sigma_0^{(i)} \right) \\ & - \sum_{i < j} \left(- \sigma_0^{(i)} \sigma_0^{(j)} - \sigma_1^{(i)} \sigma_1^{(j)} \right. \\ & \quad \left. + \sigma_0^{(i)} \sigma_1^{(j)} + \sigma_1^{(i)} \sigma_0^{(j)} \right) \geq -B_c \end{aligned} \quad (21)$$

in which the coefficients of the linear combination of single-spin and two-spin correlation functions descend from the asymptotic value of the gradient, normalized to the common absolute value of its component. Introducing the combinations

$$\mathcal{S}_a = \sum_i \sigma_a^{(i)} \quad \mathcal{S}_{ab} = \sum_{i \neq j} \sigma_a^{(i)} \sigma_b^{(j)} \quad (22)$$

with $a, b = (0, 1)$, the above Bell inequality takes the form

$$- \mathcal{S}_0 - \mathcal{S}_1 + \frac{1}{2} \mathcal{S}_{00} + \frac{1}{2} \mathcal{S}_{11} - \mathcal{S}_{01} \geq -B_c \quad (23)$$

which corresponds to the many-body Bell inequality derived by Ref. [17], with classical bound $B_c = 2N$. The saturation of the gradient to a finite value implies that the quantum data violate this Bell inequality: introducing the Bell operator

$$\hat{\mathcal{B}} = -\hat{\mathcal{S}}_0 - \hat{\mathcal{S}}_1 + \frac{1}{2} \hat{\mathcal{S}}_{00} + \frac{1}{2} \hat{\mathcal{S}}_{11} - \hat{\mathcal{S}}_{01} \quad (24)$$

with $\hat{\mathcal{S}}_a = \sum_i \hat{\sigma}_a^{(i)}$ and $\hat{\mathcal{S}}_{ab} = \sum_{i \neq j} \hat{\sigma}_a^{(i)} \hat{\sigma}_b^{(j)}$, one obtains $\langle \hat{\mathcal{B}} \rangle / N = -2.0849\dots$ on the 6×6 lattice, $-2.127\dots$ on the 8×8 lattice, $-2.147\dots$ on the 10×10 lattice, etc. namely a consistent violation of the Bell inequality becoming stronger with increasing system size – this is due to the relationship between the Bell inequality violation and squeezing [27], and to the increasing level of squeezing that larger lattices exhibit at the quantum Ising critical point [30]. The quantum data are obtained via quantum Monte Carlo simulations [30] at temperatures sufficiently low to eliminate thermal effects.

Our result is therefore two-fold: 1) the one-spin and two-spin correlation functions of the quantum critical point of the $2d$ quantum Ising model on the square lattice violate the Bell inequality of Ref. [17], Eq. (23); but also 2) among all the Bell inequalities that the quantum data at hand could violate, Eq. (23) is the one that is maximally violated, corresponding to the facet of the local polytope which is closest to the quantum data. This is a remarkable fact, given that the inequality

of Eq. (23) is symmetric under permutation of all sites, while the quantum data are *not* – indeed the correlation functions $C_{xx}^{(ij)}$ and $C_{yy}^{(ij)}$ have a strong spatial decay, which is a hallmark of quantum criticality. This result vindicates the choice of Ref. [17] to restrict the search of Bell inequalities to permutationally symmetric ones, as the latter appear to be highly relevant even to quantum data which do not share the same symmetry. The same conclusion can be drawn from the example discussed in the following sections.

C. Distilling the Bell inequality out of the numerical data

The above example gives us a prescription on how to extract the violated Bell inequality out of the numerical data for the gradient of the cost function. In practice such data are noisy (as clearly shown in Fig. 4): yet, after convergence is reached, a partial average of the gradient components over the last iteration steps strongly reduces the noise, and makes the pattern of the gradient components more explicit. In order to obtain relevant Bell inequalities that transcend the numerical uncertainty of the variational search, it is completely acceptable to guess some regularity in the coefficients of the inequality: once the inequality is reconstructed and the classical bound is obtained, the only metric of success of the whole operation is the violation of the inequality by the quantum data. This is also the procedure that led us to the results described in the sections that follow.

III. PROOF OF THE MANY-BODY PEARLE-BRAUNSTEIN-CAVES (PBC) INEQUALITY

We consider a $(N, k, 2)$ Bell scenario with $k \geq 3$, where each of the N parties has k possible measurement settings. Introducing the quantities \mathcal{S}_{ab} as in equation Eq. (22), we will prove the following Bell inequality:

$$\mathcal{B} = \sum_{a=0}^{k-1} \mathcal{S}_{aa} + \sum_{a=0}^{k-2} \mathcal{S}_{a,a+1} - \mathcal{S}_{k-1,0} \geq -2N(k-1) := -B_c, \quad (25)$$

where $-B_c$ is the classical bound. We define the collective variables $X_a = \sum_{i=1}^N \sigma_a^{(i)}$, so that $\mathcal{S}_{ab} = X_a X_b - \sum_{i=1}^N \sigma_a^{(i)} \sigma_b^{(i)}$. We then define the quantities

$$\begin{aligned} A &= \sum_{a=0}^{k-1} X_a^2 + \sum_{a=0}^{k-2} X_a X_{a+1} - X_{k-1} X_0, \\ B &= \sum_{i=1}^N \left[\sum_{a=0}^{k-2} \sigma_a^{(i)} \sigma_{a+1}^{(i)} - \sigma_{k-1}^{(i)} \sigma_0^{(i)} \right], \end{aligned} \quad (26)$$

so that:

$$\mathcal{B} = A - B - kN. \quad (27)$$

For all configurations of the variables $\sigma_a^{(i)} = \pm 1$, we have $B \leq N(k-2)$, so that $-B - kN \geq -2N(k-1)$. In order to

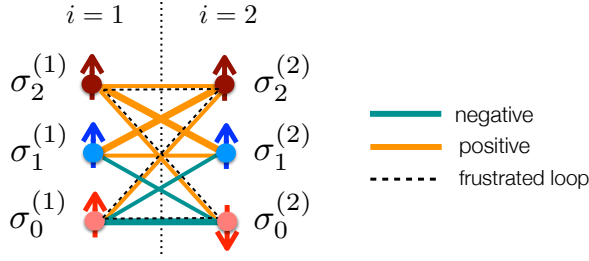


FIG. 5: Correlation pattern in a spin singlet (after π rotation around the z axis of *e.g.* qubit 1) for the local measurements indicated in Eq. (29). Orange (green) lines indicate positive (negative) correlations present in the quantum state. The dashed line marks one out of the four frustrated loops of correlations present in the quantum data.

prove Eq. (25) it is therefore enough to prove that $A \geq 0$. We introduce the notation $\vec{u} = (X_0, X_1, \dots, X_{k-1})$, so that $A = \vec{u} M \vec{u}^T$, with $M = \mathbb{1} + M'/2$, where M' is the symmetric matrix (in the Dirac notation for vectors):

$$M' = \sum_{a=0}^{k-2} |a\rangle \langle a+1| - |k-1\rangle \langle 0| + \text{h.c.} \quad (28)$$

In order to prove that $A \geq 0$, it is enough to prove that the eigenvalues ϵ_q ($q = 0, \dots, k-1$) of M' satisfy $\epsilon_q \geq -2$, so that $\vec{u} M \vec{u}^T \geq 0$ for any \vec{u} . The diagonalization of M' is achieved in two steps: 1) a local phase transformation $|\tilde{a}\rangle = e^{i\pi a/k} |a\rangle$; and 2) a Fourier transformation $|\psi_q\rangle = (1/\sqrt{k}) \sum_{a=0}^{k-1} e^{2i\pi a q/k} |\tilde{a}\rangle$. The eigenvalues of M' are $\epsilon_q = 2 \cos[\pi(2q+1)/k] \geq -2$, completing the proof that $A \geq 0$. The bound is tight for N even, as $A = 0$ is achieved with configurations $\sigma_a^{(i)}$ such that $X_a = 0$ for all a , namely, with $\sigma_a^{(i)} = 1$ for $i = 1, \dots, N/2$ and $\sigma_a^{(i)} = -1$ for $i = N/2 + 1, \dots, N$.

IV. VIOLATION OF THE MANY-BODY PBC INEQUALITY BY QUANTUM DATA

A. How quantum antiferromagnetism achieves frustration of local-variable theories for $k \geq 3$

Before diving into the formal demonstration of the violation of the Bell inequality in Eq. (25) by quantum data, it is useful to have a grasp of the physical reason behind this violation, which is also the guiding principle that allows one to identify a relevant measurement strategy on the quantum data that may lead to unveil non-locality.

Here we shall focus on the simple case of a singlet state shared by two qubits, and on the Bell scenario $(2, 3, 2)$ in which each qubit is subject to the following $k = 3$ measurements

$$\begin{aligned} \hat{\sigma}_0 &= \hat{\sigma}_x \\ \hat{\sigma}_1 &= \cos \theta \hat{\sigma}_x + \sin \theta \hat{\sigma}_y \\ \hat{\sigma}_2 &= \cos(2\theta) \hat{\sigma}_x + \sin(2\theta) \hat{\sigma}_y. \end{aligned} \quad (29)$$

To make the argument most explicit, we shall take a π rotation around the x axis *e.g.* the qubit 1, so that the correlations in the quantum state are $-1 = \langle \hat{\sigma}_x^{(1)} \hat{\sigma}_x^{(2)} \rangle = -\langle \hat{\sigma}_y^{(1)} \hat{\sigma}_y^{(2)} \rangle$. The quantum data of interest are represented by the correlation functions among all possible measurements on the two qubits, $C_{ab} = \langle \sigma_a^{(1)} \sigma_b^{(2)} \rangle_Q$, which take values:

$$\begin{aligned} C_{00} &= -1 \\ C_{11} &= -\cos(2\theta) \\ C_{22} &= -\cos(4\theta) \\ C_{01} = C_{10} &= -\cos \theta \\ C_{02} = C_{20} &= -\cos(2\theta) \\ C_{12} = C_{21} &= -\cos(3\theta). \end{aligned} \quad (30)$$

Choosing (as we shall do in the following) $\theta = \pi/3$ produces the simple correlation pattern $C_{00} = -C_{12} = -1$, $C_{11} = C_{02} = C_{22} = -C_{01} = 1/2$. This correlation pattern is pictured in Fig. 5: it exhibits four frustrated correlation loops – characterized by the presence of an odd number of correlations of the same sign – such as in the loop $\sigma_0^{(1)} \rightarrow \sigma_0^{(2)} \rightarrow \sigma_2^{(1)} \rightarrow \sigma_2^{(2)} \rightarrow \sigma_0^{(1)}$. This implies that the effective Hamiltonian for an LV theory capable of reproducing (or at least approaching) this correlation pattern between antiferromagnetically correlated spins must necessarily be frustrated. In fact the very correlation pattern of Eq. (30) for two spins and $\theta = \pi/3$ is already impossible to reproduce with an LV theory. This aspect is at the heart of the violation of the Pearle-Braunstein-Caves inequality [31, 32] for two qubits.

B. Coplanar measurement axes

To test the violation of the Bell inequality Eq. (25) by a quantum state, we introduce the Bell operator for N spins

$$\hat{B} = \sum_{a=0}^{k-1} \hat{S}_{aa} + \sum_{a=0}^{k-2} \hat{S}_{a,a+1} - \hat{S}_{k-1,0}. \quad (31)$$

where $\hat{S}_{ab} = \sum_{i \neq j} \hat{\sigma}_i^{(a)} \hat{\sigma}_j^{(b)}$.

In order to achieve the maximal violation of the above Bell inequality in the $(N, k, 2)$ scenario by a set of quantum data, one should in principle optimize freely over all k measurement axes. Pursuing this exhaustive search would lead to extremizing a complex function of $2k$ angles specifying the orientations of all measurement axes. While this is entirely feasible, we opt for a more practical scheme by which we restrict the search to the situation in which all measurement axes are co-planar and form an angle θ between consecutive axes; in other words, the measurement operators correspond to

$$\hat{\sigma}_a = \cos(\theta a) \hat{\sigma}_x + \sin(\theta a) \hat{\sigma}_y \quad (a = 0, \dots, k-1) \quad (32)$$

generalizing the scheme proposed in Eq. (29). Without loss of generality, we choose the xy plane as the measurement plane and $\hat{\sigma}_0 = \hat{\sigma}_x$.

The above choice of measurement axes is rather natural: consecutive measurement axes are coupled pairwise in the

same way in the Bell operator $\hat{\mathcal{B}}$ (except for the last and the first one), and therefore they should form the same angles with each other, not necessarily in the same plane. The choice of coplanarity is motivated by the attempt to maximally exploit the correlations present in the the potential quantum states: indeed, having fixed the orientations of the first (0-th) and last $((k-1)$ -th) measurement axes, which define the plane of interest, the other measurement axes are maximally close to each other (and therefore give rise to maximally correlated measurements) if they are chosen to lie in that same plane.

C. Expectation value of the Bell operator

Having parametrized the choice of the measurement axes uniquely by the angle θ , our goal is then to minimize the function $\langle \hat{\mathcal{B}} \rangle(\theta)$ when calculating it for a specific quantum state. Following the treatment of the Bell inequality in Sec. III, we rewrite the $\hat{\mathcal{S}}$ operators in terms of the collective spin operators $\hat{J}_a = \sum_i \hat{S}_a^{(i)}$ as

$$\hat{\mathcal{S}}_{ab} = 2 \left(\hat{J}_a \hat{J}_b + \hat{J}_b \hat{J}_a \right) - \frac{1}{2} \sum_i \left(\hat{\sigma}_a^{(i)} \hat{\sigma}_b^{(i)} + \hat{\sigma}_b^{(i)} \hat{\sigma}_a^{(i)} \right). \quad (33)$$

As a consequence, the Bell operator can be rewritten as

$$\hat{\mathcal{B}} = \hat{A} - \hat{B} - kN \quad (34)$$

where

$$\begin{aligned} \hat{A} = & 4 \sum_{a=0}^{k-1} \hat{J}_a^2 + 2 \sum_{a=0}^{k-2} \left(\hat{J}_a \hat{J}_{a+1} + \hat{J}_{a+1} \hat{J}_a \right) \\ & - 2 \left(\hat{J}_{k-1} \hat{J}_0 + \hat{J}_0 \hat{J}_{k-1} \right) \end{aligned} \quad (35)$$

and

$$\begin{aligned} \hat{B} = & \frac{1}{2} \sum_{a=0}^{k-2} \sum_{i=1}^N \left(\hat{\sigma}_a^{(i)} \hat{\sigma}_{a+1}^{(i)} + \hat{\sigma}_{a+1}^{(i)} \hat{\sigma}_a^{(i)} \right) \\ & - \frac{1}{2} \left(\hat{\sigma}_{k-1}^{(i)} \hat{\sigma}_0^{(i)} + \hat{\sigma}_0^{(i)} \hat{\sigma}_{k-1}^{(i)} \right) \end{aligned} \quad (36)$$

where we have used the fact that $\hat{\sigma}_a^2 = \mathbb{1}$. Given that $\hat{J}_a = \cos(\theta a) \hat{J}_x + \sin(\theta a) \hat{J}_y$, straightforward algebra leads to rewriting the components of the Bell operator in terms of the operators \hat{J}_x^2 , \hat{J}_y^2 and $\hat{J}_x \hat{J}_y + \hat{J}_y \hat{J}_x$ as follows:

$$\hat{A} = F_x(\theta) \hat{J}_x^2 + F_y(\theta) \hat{J}_y^2 + F_{xy}(\theta) \left(\hat{J}_x \hat{J}_y + \hat{J}_y \hat{J}_x \right) \quad (37)$$

with

$$\begin{aligned} F_x(\theta) = & 2k + 2(k-1) \cos(\theta) - 4 \cos[(k-1)\theta] \\ & + 1 + \frac{1}{\sin \theta} \{ \sin[(2k-1)\theta] + \sin[2(k-1)\theta] \} \\ F_y(\theta) = & 2k + 2(k-1) \cos(\theta) \\ & - 1 - \frac{1}{\sin \theta} \{ \sin[(2k-1)\theta] + \sin[2(k-1)\theta] \} \\ F_{xy}(\theta) = & -2 \sin[(k-1)\theta] + \frac{1}{\sin \theta} \left\{ 1 + \cos \theta \right. \\ & \left. - \cos[(2k-1)\theta] - \cos[2(k-1)\theta] \right\} \end{aligned} \quad (38)$$

A similar calculation leads to the explicit form of the \hat{B} operator, which turns out to be simply proportional to the identity, $\hat{B} = G(\theta)N$, with

$$G(\theta) = (k-1) \cos \theta - \cos[(k-1)\theta] \quad (39)$$

Therefore the angle θ can be found by minimizing the expectation value of the Bell operator on the quantum state of interest

$$\begin{aligned} \langle \hat{\mathcal{B}} \rangle(\theta) = & F_x(\theta) \langle \hat{J}_x^2 \rangle + F_y(\theta) \langle \hat{J}_y^2 \rangle \\ & + F_{xy}(\theta) \langle \hat{J}_x \hat{J}_y + \hat{J}_y \hat{J}_x \rangle - N(G(\theta) + k) \end{aligned} \quad (40)$$

in order to satisfy the condition (Bell inequality violation) $\langle \hat{\mathcal{B}} \rangle < -2N(k-1)$.

The above formula is completely general and it relies uniquely on the choice of coplanar measurement axes, forming equal angles between consecutive axes. In the following we shall specialize it to $U(1)$ symmetric states.

D. Bell operator for $U(1)$ -symmetric states

In the case of $U(1)$ -symmetric states, invariant under a rotation around the z axis, one has that $\langle \hat{J}_x \hat{J}_y + \hat{J}_y \hat{J}_x \rangle = 0$ and $\langle \hat{J}_x^2 \rangle = \langle \hat{J}_y^2 \rangle$, so that the expectation value of the Bell operator reduces to

$$\langle \hat{\mathcal{B}} \rangle(\theta) = F(\theta) \langle \hat{J}_x^2 \rangle - N(G(\theta) + k) \quad (41)$$

where

$$\begin{aligned} F(\theta) = & F_x(\theta) + F_y(\theta) \\ = & 4[k + (k-1) \cos \theta - \cos[(k-1)\theta]] \\ = & 4[k + G(\theta)] \end{aligned} \quad (42)$$

The violation of the Bell inequality is then achieved under the condition

$$\frac{\langle \hat{J}_x^2 \rangle}{N} < \frac{1}{4} - \frac{2(k-1)}{F(\theta)}. \quad (43)$$

A maximal violation of the Bell inequality can therefore be achieved upon maximizing the right-hand side, which implies maximising the F function since $k \geq 3$. This maximum is achieved for $\theta = \pi/k$, and it takes the value

$$F_{\max} = F(\pi/k) = k \left(1 + \cos \frac{\pi}{k} \right). \quad (44)$$

Hence the optimal witness condition for Bell non-locality of $U(1)$ symmetric states takes the form:

$$\frac{\langle \hat{J}_x^2 \rangle}{N} < \beta_k = \frac{2 - k + k \cos \frac{\pi}{k}}{4k \left(1 + \cos \frac{\pi}{k} \right)}. \quad (45)$$

We find the following bounds: $\beta_3 = 1/36 = 0.027777\dots$, $\beta_4 = 1/(16 + 12\sqrt{2}) = 0.030330\dots$, $\beta_5 = 0.028885$, etc. The largest bound for the witness inequality Eq. (45) is therefore obtained for $k = 4$. This is the inequality we used in the main text to probe non-locality in the low-temperature states of Heisenberg antiferromagnets.

V. MAXIMAL QUANTUM VIOLATION OF THE PBC INEQUALITY

In the measurement setting we have described, the maximal violation of Eq. (25) is obtained when $\langle \hat{J}_x^2 \rangle = 0$ in a $U(1)$ symmetric state – implying that one is actually dealing with a global singlet with higher ($SU(2)$) symmetry. The above conditions yields $\langle \hat{\mathcal{B}} \rangle = -Nk[1 + \cos(\pi/k)] < -B_c$ [see Eq. (41)]. We now prove that $-B_q := -Nk[1 + \cos(\pi/k)]$ is the maximal violation of the Bell inequality Eq. (25) allowed by quantum mechanics. Specifically, we will show that

$$\hat{\mathcal{B}} + B_q \mathbb{1} \geq 0, \quad (46)$$

namely that all eigenvalues of $\hat{\mathcal{B}} + B_q \mathbb{1}$ are non-negative, by rewriting this operator as a sum of squares. To define the Bell operator $\hat{\mathcal{B}}$, we first introduce the operators $\hat{X}_a = \sum_{i=1}^N \hat{\sigma}_a^{(i)}$, and $\hat{\mathcal{S}}_{ab} = (1/2)\{\hat{X}_a, \hat{X}_b\} - (1/2)\sum_{i=1}^N \{\hat{\sigma}_a^{(i)}, \hat{\sigma}_b^{(i)}\}$, with the anti-commutator $\{\hat{A}, \hat{B}\} = \hat{A}\hat{B} + \hat{B}\hat{A}$. The only property of the $\hat{\sigma}_a^{(i)}$ operators that we require is that they be hermitians, and that $(\hat{\sigma}_a^{(i)})^2 = \mathbb{1}$, namely, that their measurement outputs ± 1 , regardless of the number of dimensions of the local Hilbert space upon which they act.

The Bell operator is then defined as in Eq. (31), yet with a generalized definition for the $\hat{\sigma}_a^{(i)}$ operators entering into the $\hat{\mathcal{S}}_{ab}$ operators. The Bell operator is a quadratic form in the $\hat{\sigma}_a^{(i)}$ operators. We make this form explicit by introducing the vectors of operators $\hat{\vec{X}} = (\hat{X}_0, \dots, \hat{X}_{k-1})$ and $\hat{\vec{\sigma}}^{(i)} = (\hat{\sigma}_0^{(i)}, \dots, \hat{\sigma}_{k-1}^{(i)})$. Using the matrix M' introduced in

Eq. (28), we have:

$$\begin{aligned} \hat{\mathcal{B}} + B_q \mathbb{1} &= \hat{\vec{X}}^T \left[\mathbb{1} + \frac{1}{2} M' \right] \hat{\vec{X}} \\ &+ \sum_{i=1}^N (\hat{\vec{\sigma}}^{(i)})^T \left[\left(\frac{B_q}{Nn} - 1 \right) \mathbb{1} - \frac{1}{2} M' \right] \hat{\vec{\sigma}}^{(i)}, \end{aligned} \quad (47)$$

where we use that $(\hat{\vec{\sigma}}^{(i)})^T \cdot \hat{\vec{\sigma}}^{(i)} = \sum_{a=0}^{k-1} (\hat{\sigma}_a^{(i)})^2 = k \mathbb{1}$. The symmetric matrix M' has been diagonalized in Sec. III, so that $U^\dagger M' U = \text{diag}(\epsilon_0, \dots, \epsilon_{k-1})$ with $\epsilon_q = 2 \cos[\pi(2q + 1)/k]$. Introducing the operators $\hat{\vec{Y}} = \hat{\vec{X}} U^\dagger$ and $\hat{\vec{\tau}}_i = \hat{\vec{\sigma}}_i U^\dagger$, we obtain:

$$\begin{aligned} \hat{\mathcal{B}} + B_q \mathbb{1} &= \sum_{a=1}^n \left[1 + \frac{\epsilon_a}{2} \right] \hat{\vec{Y}}_a^\dagger \hat{\vec{Y}}_a \\ &+ \sum_{i=1}^N \sum_{a=1}^n \left[\frac{B_q}{Nn} - 1 - \frac{\epsilon_a}{2} \right] (\hat{\vec{\tau}}_a^{(i)})^\dagger \hat{\vec{\tau}}_a^{(i)}. \end{aligned} \quad (48)$$

We have $1 + \epsilon_a/2 \geq 0$ for all a , and if we choose $B_q = Nn[1 + \max_a \epsilon_a/2] = Nn[1 + \cos(\pi/n)]$, we achieve a sum-of-squares decomposition, implying that for *any* Hilbert space size, and *any* wavefunction $|\Psi\rangle$, we have:

$$\langle \Psi | \hat{\mathcal{B}} | \Psi \rangle \geq -B_q. \quad (49)$$

The measurement protocol we have proposed on a many-body spin singlet, achieving $\langle \mathcal{B} \rangle = -B_q$, yields therefore the maximal violation of the Bell inequality Eq. (25) allowed by quantum mechanics.